

# Crystal structure, phase transitions and vibrations of H<sub>2</sub>O molecules in [Ca(H<sub>2</sub>O)<sub>2</sub>](ReO<sub>4</sub>)<sub>2</sub>

Joanna Hetmańczyk<sup>1,2</sup> · Łukasz Hetmańczyk<sup>1,2</sup> · Wojciech Nitek<sup>2</sup>

Received: 4 November 2016 / Accepted: 22 May 2017 / Published online: 6 June 2017  
© The Author(s) 2017. This article is an open access publication

**Abstract** One reversible phase transition at  $T_c^h = 261.2$  K (upon heating) was observed for [Ca(H<sub>2</sub>O)<sub>2</sub>](ReO<sub>4</sub>)<sub>2</sub> in the 120–300 K range. Thermal hysteresis of the phase transition temperature  $T_C$  of ca. 30 K and heat flow anomaly sharpness suggest that the detected phase transition is of a first-order type. The entropy change value ( $\Delta S \approx 1.6 \pm 0.08$  J mol<sup>-1</sup> K<sup>-1</sup>), associated with the observed phase transition (PT), indicates a moderate degree of molecular dynamical disorder. X-ray single crystal and neutron powder diffraction measurements indicated that the crystal space group (I 2/a) is the same for the high- and low-temperature phases. However, FT-IR and RS spectra show a narrowing (during sample cooling) of the bands connected with vibrations of the H<sub>2</sub>O molecules and ReO<sub>4</sub><sup>-</sup> ions. This suggests that the anions and the ligands from the complex cation perform rapid (picosecond correlation time scale, which is characteristic of optical spectroscopy) stochastic reorientational motions in the low- and high-temperature phases. Moreover, apart from the narrowing, the splitting of some bands can be seen below the phase transition.

**Keywords** Diaquacalcium rhenate(VII) · Thermal decomposition (TG/QMS) · Phase transition · DSC · X-ray single crystal and neutron powder diffraction (XRSCD, NPD) · Fourier transform middle- and far-infrared spectroscopy (FT-MIR and FT-FIR)

## Introduction

Diaquacalcium rhenate(VII), with the formula [Ca(H<sub>2</sub>O)<sub>2</sub>](ReO<sub>4</sub>)<sub>2</sub>, is a particularly interesting molecular material, because of the occurrence of reorientational motions of the H<sub>2</sub>O ligands, ReO<sub>4</sub><sup>-</sup> anions and the whole [Ca(H<sub>2</sub>O)<sub>2</sub>]<sup>2+</sup> complex cations. Similar compounds with the same ligand [1–3] and anion [4, 5] exhibit also an interesting polymorphism.

At room temperature (RT), diaquacalcium rhenate(VII) crystallises in the centrosymmetric monoclinic system (space group C2/c, No. = 15) with the unit cell parameters:  $a = 18.8975(2)$  Å,  $b = 7.0720(2)$  Å,  $c = 14.1910(2)$  Å,  $\alpha = \beta = 90^\circ$ ,  $\gamma = 115.38^\circ$  and with eight molecules per unit cell ( $Z = 8$ ) [6]. However, in the literature one can find that this compound crystallises in noncentrosymmetric monoclinic space group Cc [7] or C2 [8]. The ReO<sub>4</sub><sup>-</sup> anions have a mostly regular tetrahedral geometry with an average Re–O bond length of 1.72 Å [7]. The calcium atoms in this structure are surrounded by eight oxygen atoms with an average Ca–O distance of  $\sim 2.46$  Å. The Ca<sub>2</sub>(H<sub>2</sub>O)<sub>4</sub>O<sub>10</sub> polyhedral long-chain structure is formed [6–8].

The polymorphism of the above-mentioned compound was investigated by us (unpublished data) by means of differential scanning calorimetry. The measurements were performed in the temperature range of 300–120 K on cooling and heating of the sample at different rates.

**Electronic supplementary material** The online version of this article (doi:10.1007/s10973-017-6494-y) contains supplementary material, which is available to authorized users.

✉ Joanna Hetmańczyk  
serwonsk@chemia.uj.edu.pl

<sup>1</sup> Frank Laboratory of Neutron Physics, Joint Institute for Nuclear Research, Dubna, Russian Federation 141980

<sup>2</sup> Department of Chemical Physics, Faculty of Chemistry, Jagiellonian University, ul. Ingardena 3, 30-060 Cracow, Poland

It was thought interesting to see whether a compound of the same type (with  $\text{H}_2\text{O}$  ligands or  $\text{ReO}_4^-$  anions) will possess a phase polymorphism similar to that of those compounds just mentioned. The general aim of the present study is to investigate the polymorphism of  $[\text{Ca}(\text{H}_2\text{O})_2](\text{ReO}_4)_2$  in the temperature range of 120–300 K and find the connections of recorded phase transition with eventual changes of the crystal structure and/or of the rate of stochastic reorientational motions of  $\text{H}_2\text{O}$  ligands.

For this purpose, we employed differential scanning calorimetry (DSC), Fourier transform far- and middle-infrared spectroscopy (FT-FIR and FT-MIR), X-ray single crystal diffraction (XRSCD) and neutron powder diffraction (NPD) measurements. The optical spectroscopy methods provide information on fast reorientational ( $\tau_R$  is of an order: from  $10^{-11}$  to  $10^{-13}$  s) molecular motions.

In addition, we would like to obtain a better understanding of mechanisms of thermal decomposition of the title compound, particularly of its dehydration processes.

## Experimental

The examined compound  $[\text{Ca}(\text{H}_2\text{O})_2](\text{ReO}_4)_2$  was obtained by treating calcium carbonate (bought from the Sigma-Aldrich company) with water-diluted perhenic acid. The solution was concentrated by mild heating, and colourless crystals, obtained after cooling the solution, were purified by repeated crystallisation from four-time distilled water. Then, the crystals were dried for several days in a desiccator over BaO. The composition of the investigated compound was determined based on its calcium content by titration using EDTA. The average calcium content was found to be equal to the theoretical value for  $[\text{Ca}(\text{H}_2\text{O})_2](\text{ReO}_4)_2$  within an error margin of  $\pm 0.79\%$ .

X-ray diffraction intensity measurements (XRSCD) performed for the single crystal sample at 293 and 105 K were carried out on a Nonius Kappa CCD diffractometer equipped with a molybdenum X-ray tube and Oxford Cryostream cooler. The same data collection strategy (complete sphere of reciprocal space, 6 s exposure time) was used for each of these two experiments. The collected data were processed using DENZO-SCALEPACK [9]. The phase problem was solved using the SIR-92 programme [10], and the refinement was performed with the SHELXL-97 programme [11]. The positions of the hydrogen atoms were located from the difference Fourier maps and refined positionally with individual isotropic thermal parameters. All non-H atoms were refined anisotropically.

Thermal analysis was performed using thermogravimetry and differential thermal analysis methods (TG/SDTA) with the aid of *Mettler-Toledo 851<sup>e</sup>* apparatus. The sample of mass 56.3779 mg was placed in a 150- $\mu\text{L}$  open

corundum crucible. The measurements were made in a flow of argon ( $60 \text{ mL min}^{-1}$ ), within a temperature range of 295–1085 K. The TG measurements were performed at a constant heating rate of  $5 \text{ K min}^{-1}$ . The simultaneous evolved gas analysis (SEGA) was performed during the experiments by a joined on-line quadruple mass spectrometer (QMS) using a Thermostat-Balzers apparatus. The temperature was measured by a Pt–Pt/Rh thermocouple with an accuracy of  $\pm 0.5 \text{ K}$ .

Differential scanning calorimetry (DSC) measurements in the temperature range of 310–1500 K were performed using a *Mettler-Toledo 821<sup>e</sup>* calorimeter. The sample of mass equal to 10.88 mg was placed in 40- $\mu\text{L}$  aluminium open crucible, under constant flow of argon ( $80 \text{ mL min}^{-1}$ ), with the heating rate equal to  $10 \text{ K min}^{-1}$ . The DSC measurements below room temperature were taken using a *Mettler-Toledo 822<sup>e</sup>* calorimeter. Sample of mass 12.43 mg was placed in an aluminium container and closed by compression. Another empty vessel was used as a reference. The instrument was calibrated by means of the melting points of indium and water for the high- and low-temperature region, respectively. The DSC measurements were taken during both heating and cooling of the sample at constant rates of 10 and  $20 \text{ K min}^{-1}$  for the sample. The enthalpy change ( $\Delta H$ ) was calculated by the numerical integration of the DSC curve under the anomaly peak after a linear background arbitrary subtraction. The entropy change ( $\Delta S$ ) was calculated using the formula  $\Delta S = \Delta H/T_C$ . Other experimental details were the same as those published in our previous paper [12].

Fourier transforms far- and middle-infrared (FT-FIR, FT-MIR) absorption measurements were performed using a *Bruker Vertex 70v* vacuum Fourier transform spectrometer. The transmission spectra were collected with a resolution of  $2 \text{ cm}^{-1}$  and with 32 scans per each spectra for FT-FIR and FT-MIR, respectively. The FT-FIR spectra ( $500\text{--}50 \text{ cm}^{-1}$ ) were collected for a sample suspended in Apiezon N grease and placed on a polyethylene (PE) disc. The FT-MIR spectra were collected for sample suspended in Nujol between KBr pellets. The Apiezon and Nujol additionally preserve the sample from decomposition and the influence of atmospheric conditions. Temperature measurements were carried out using *Advanced Research System cryostat DE-202A* and a water-cooled helium compressor *ARS-2HW* working in a closed cycle manner. The sample was loaded at room temperature, and measurements were taken on cooling down to ca. 9 K. The desired temperature was measured with an accuracy of  $\pm 0.1 \text{ K}$  and stabilised for ca. 3 min before the measurements were taken. The *LakeShore 331S* temperature controller equipped with silicon diode sensor was used to control the temperature. The cooling rate between desired temperatures was ca.  $3 \text{ K min}^{-1}$ . The PE and KRS5

**Table 1** Experimental details and results of X-ray diffraction measurements

Temperature	293.0(2) K	105.0(2) K
Empirical formula	[Ca(H <sub>2</sub> O) <sub>2</sub> ](ReO <sub>4</sub> ) <sub>2</sub>	
Formula weight	576.51 g mol <sup>-1</sup>	
Crystal system	Monoclinic	
Space group	I 2/a	
Unit cell dimensions	$a = 18.1302(7) \text{ \AA}$ $\alpha = 90.000(5)^\circ$ $b = 7.07220(2) \text{ \AA}$ $\beta = 109.637(4)^\circ$ $c = 14.1882(5) \text{ \AA}$ $\gamma = 90.000(5)^\circ$	$a = 18.1160(4) \text{ \AA}$ $\alpha = 90.000(5)^\circ$ $b = 7.01260(10) \text{ \AA}$ $\beta = 110.386(2)^\circ$ $c = 14.1104(3) \text{ \AA}$ $\gamma = 90.000(5)^\circ$
Volume	1713.41(11) Å <sup>3</sup>	1680.31(6) Å <sup>3</sup>
Z	8	
Density (calculated)	4.470 Mg m <sup>-3</sup>	4.558 Mg m <sup>-3</sup>
Wavelength	0.71073 Å	
Absorption coefficient	28.863 mm <sup>-1</sup>	29.431 mm <sup>-1</sup>
F(000)	2032	
Crystal size	0.459 × 0.279 × 0.089 mm <sup>3</sup>	0.442 × 0.280 × 0.084 mm <sup>3</sup>
Theta range for data collection	from 3.049° to 28.689°	from 3.080° to 28.703°
Index ranges	-24 ≤ h ≤ 24, -9 ≤ k ≤ 9 -19 ≤ l ≤ 18	
Reflections collected	10,245	10,677
Independent reflections	2075 [R(int) = 0.1306]	2028 [R(int) = 0.0826]
Completeness to theta = 25.242°	99.9%	99.6%
Absorption correction	Semi-empirical from equivalents	
Refinement method	Full-matrix least-squares on F <sup>2</sup>	
Data/restraints/parameters	2075/0/118	2028/0/119
Goodness of fit on F <sup>2</sup>	1.085	1.084
Final R indices [I > 2σ(I)]	R <sub>1</sub> = 0.0876, wR <sub>2</sub> = 0.2245	R <sub>1</sub> = 0.0322, wR <sub>2</sub> = 0.0688
R indices (all data)	R <sub>1</sub> = 0.0937, wR <sub>2</sub> = 0.2358	R <sub>1</sub> = 0.0359, wR <sub>2</sub> = 0.0707
Extinction coefficient	n/a	0.00263(7)
Largest diff. peak and hole	5.341 and -5.061 e Å <sup>-3</sup>	3.636 and -3.727 e Å <sup>-3</sup>

windows were used in a cryostat in the case of FT-FIR and FT-MIR measurements, respectively.

The neutron powder diffraction (NPD) patterns were measured using the time-of-flight method on a NERA spectrometer [13] at the high-flux pulsed reactor IBR-2 in Dubna (Russia) at temperatures 10, 200, 250 and 295 K. Experimental details are the same as in our previous paper [14].

## Results and discussion

### Crystal structure of [Ca(H<sub>2</sub>O)<sub>2</sub>](ReO<sub>4</sub>)<sub>2</sub> at 293 and 105 K

#### X-ray single crystal diffraction

X-ray diffraction intensity measurements were performed for the single crystal sample at 293 K (high-temperature phase—phase I) and at 105 K (low-temperature phase—

phase II). Table 1 presents experimental details of the X-ray measurement for [Ca(H<sub>2</sub>O)<sub>2</sub>](ReO<sub>4</sub>)<sub>2</sub>. Diaquacalcium rhenate(VII) crystallises in the centrosymmetric monoclinic system in the space group I 2/a, No. = 15 with eight molecules per unit cell (Z = 8) in the high- and low-temperature phase. The structure determined at room temperature is close to that reported earlier [6]. Figure 1 shows the view of the elementary cell of [Ca(H<sub>2</sub>O)<sub>2</sub>](ReO<sub>4</sub>)<sub>2</sub> at 105 K. Each Ca<sup>2+</sup> cation coordinates three H<sub>2</sub>O molecules with a Ca<sup>2+</sup>–O distances: 2.374 and 2.512 Å and six oxygen atoms: O(3) belonging to rhenate(VII) anions ReO<sub>4</sub><sup>-</sup> with Ca<sup>2+</sup>–O distance in the range of 2.3843–2.793 Å. The ReO<sub>4</sub><sup>-</sup> anions have a mostly regular tetrahedral geometry with an average Re–O bond length of 1.72 Å. Each rhenate(VII) ion in the structure is hydrogen-bonded to water molecules. The Ca atoms in this structure are coordinated by nine O atoms. The coordination geometry of the calcium ion can be best approximated as monocapped square antiprism CaO<sub>6</sub>(H<sub>2</sub>O)<sub>3</sub>. The same

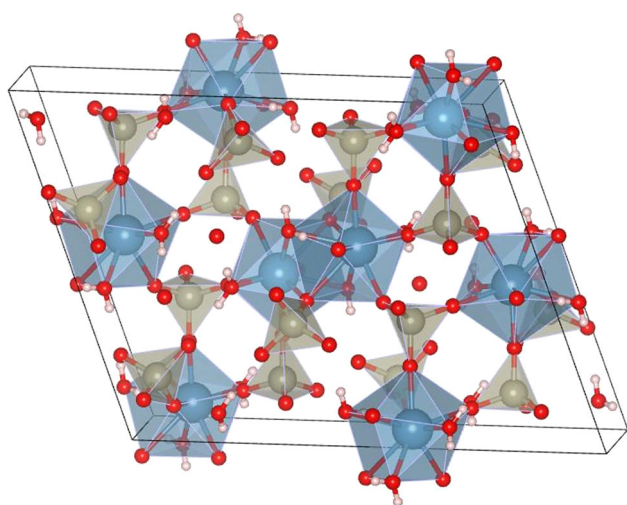


**Fig. 1** View of the unit cell of  $[\text{Ca}(\text{H}_2\text{O})_2](\text{ReO}_4)_2$  at 105 K

ninefold coordination, which can be described as a monocapped square antiprism, possesses strontium atom in  $[\text{Sr}(\text{H}_2\text{O})_6]\text{Cl}_2$  [15] and in coordination polymer  $\{[\text{Sr}(\text{C}_4\text{HO}_4)_2(\text{H}_2\text{O})_5] \cdot 0.5\text{H}_2\text{O}\}_n$  [16]. The two opposite square planes are defined by O(10)O(8)O(10)#5O(8)#4 and O(1)O(4)O(5)O(9), respectively, while O(3) can be considered as the capping atom (see Fig. 2). Figure 2 was prepared using CrystalMaker software [17] and presents two Ca cations polyhedra which are connected by diamond.

The dihedral angle between the two mean planes is  $3.05018^\circ$  at room temperature, whereas in the 105 K this angle is  $3.35065^\circ$ . Atom O3<sup>vi</sup> projects through the second of these faces to provide the cap. The Ca atom is displaced

by  $-1.814 \text{ \AA}$  from the first plane (defined by O(10)O(8)O(10)#5O(8)#4) at 105 K and by  $-1.844 \text{ \AA}$  at room temperature.

The crystal structure formed by the title compound in the low- and high-temperature phases is rather stiff. This stiffness is caused by the network of hydrogen bonds [7]. The crystal structure in both phases is very similar. However, some kind of conformational flexibility (reorientations and librations) of the anion and complex cation is also possible. Detailed geometrical parameters of diaquacalcium rhenate(VII) at room temperature, compared with appropriate parameters at a temperature of 105 K, are listed in Table 2 (fractional coordinations and  $U(\text{eq})$ ) and Table S1 (selected bond lengths, angles and torsion angles, supplementary material). These parameters are close to those reported earlier [5–7] for the structure determined at room temperature.

Comparison of the structure determined at 105 K and at room temperature (see Table 1 and Table S1) shows the differences between torsion angles in the structure of  $[\text{Ca}(\text{H}_2\text{O})_2](\text{ReO}_4)_2$  at 293 and 105 K. The interatomic distances (with the exception of Cl–O distance in the chlorate(VII) group) and atom displacement parameters are decreasing slightly, which is a natural consequence of the temperature decreasing. Geometrical details of hydrogen bonds, observed in the crystal structures determined at 293 and 105 K, are listed in Table S2 (supplementary material). We can see slight differences of the hydrogen bond network in the crystal structure of the  $[\text{Ca}(\text{H}_2\text{O})_2](\text{ReO}_4)_2$  at 293 and 105 K. This can be connected with changes in water molecule orientations.

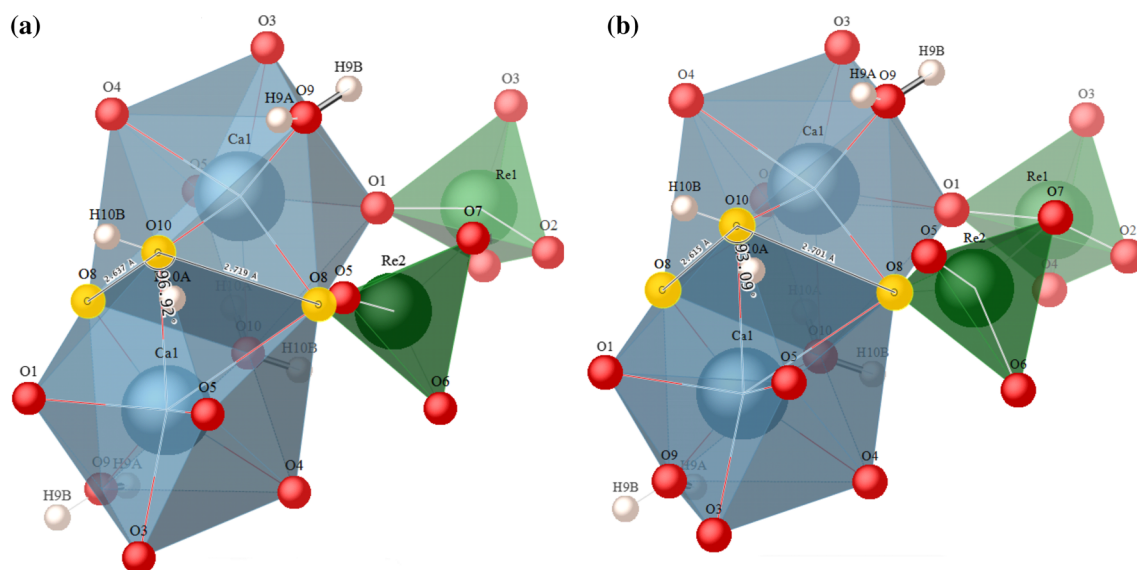


**Fig. 2** Two monocapped square antiprism geometry of the neighbouring Ca atoms in the crystal structure of  $[\text{Ca}(\text{H}_2\text{O})_2](\text{ReO}_4)_2$  at temperature: **a** 293 K and **b** 105 K

**Table 2** Atomic coordinates ( $\times 10^4$ ) and equivalent isotropic displacement parameters ( $\text{\AA}^2 \times 10^3$ ) for the structures of the [Ca(H<sub>2</sub>O)<sub>2</sub>](ReO<sub>4</sub>)<sub>2</sub> determined at temperatures 293 and 105 K

	<i>x</i>	<i>y</i>	<i>z</i>	<i>U</i> (eq)
293 K				
O(1)	3616(7)	3740(20)	2712(9)	48(3)
O(2)	3301(9)	5855(19)	922(12)	54(3)
O(3)	2296(8)	2910(20)	1020(11)	56(3)
O(4)	3792(7)	2127(18)	986(9)	44(3)
O(5)	4228(7)	720(20)	4372(9)	47(3)
O(6)	4866(8)	−110(20)	2846(10)	54(3)
O(7)	3325(10)	−930(20)	2516(12)	65(4)
O(8)	4525(9)	−3080(20)	3928(10)	59(4)
O(9)	2996(9)	6330(30)	4243(13)	68(5)
O(10)	4681(8)	6265(19)	5874(10)	47(3)
Ca(1)	3994(2)	3981(5)	4491(3)	42(1)
Re(1)	3258(1)	3643(1)	1420(1)	42(1)
Re(2)	4229(1)	−875(1)	3415(1)	43(1)
105 K				
O(1)	3600(3)	3744(8)	2720(4)	10(1)
O(2)	3284(3)	5823(9)	897(4)	12(1)
O(3)	2291(3)	2838(9)	1003(4)	10(1)
O(4)	3800(3)	1999(8)	1019(4)	9(1)
O(5)	4217(3)	682(8)	4376(4)	7(1)
O(6)	4914(3)	−28(9)	2918(4)	10(1)
O(7)	3341(3)	−1049(8)	2508(4)	10(1)
O(8)	4573(3)	−3101(9)	3963(4)	9(1)
O(9)	3048(3)	6455(9)	4253(4)	16(1)
O(10)	4679(3)	6336(8)	5900(4)	9(1)
Ca(1)	4005(1)	4010(2)	4514(1)	6(1)
Re(1)	3250(1)	3614(1)	1415(1)	5(1)
Re(2)	4250(1)	−897(1)	3436(1)	6(1)

*U*(eq) is defined as one-third of the trace of the orthogonalized  $U^{ij}$  tensor

### Neutron powder diffraction

The neutron diffraction patterns (NPD) for polycrystalline [Ca(H<sub>2</sub>O)<sub>2</sub>](ReO<sub>4</sub>)<sub>2</sub> were registered during the sample heating at four selected temperatures of measurement: 5, 200, 250 and 295 K. Figure 3 presents the NPD patterns registered at 295 K (phase I) and at 5 K (phase II) for scattering angles  $2\theta = 51.15^\circ$ . Thermal expansion is observed by increasing lattice distances; however, we cannot see any important differences between the NPD patterns obtained for all two crystalline phases. From the point of view of the neutron diffraction method, the crystal structure of [Ca(H<sub>2</sub>O)<sub>2</sub>](ReO<sub>4</sub>)<sub>2</sub> does not change (or the changes are very small) after the phase transitions. As was stated above from single crystal measurements, the crystal structure does not change in the phase transition at  $T_C$ . This

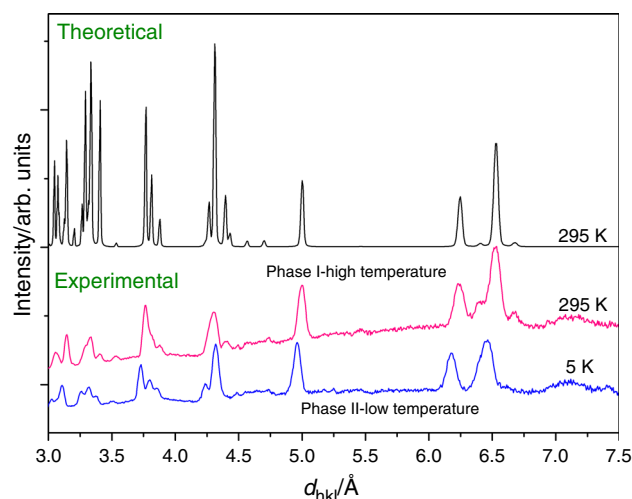


**Fig. 3** Comparison of the experimental and calculated NPD patterns of [Ca(H<sub>2</sub>O)<sub>2</sub>](ReO<sub>4</sub>)<sub>2</sub> obtained for scattering angle  $2\theta = 51.15^\circ$  at two extreme temperatures of measurements: 295 and 5 K

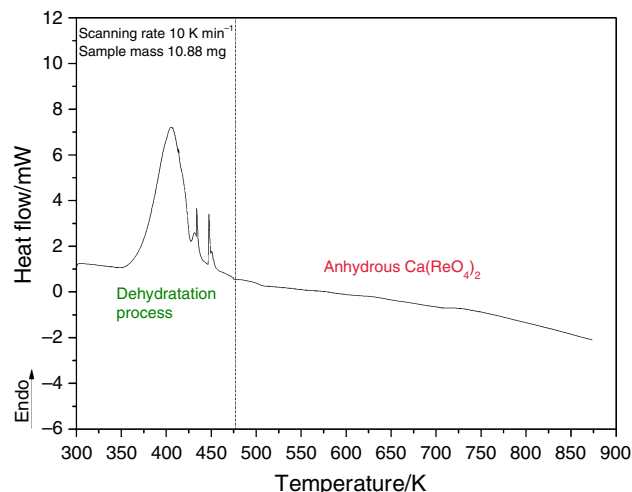


**Fig. 4** DSC curve for [Ca(H<sub>2</sub>O)<sub>2</sub>](ReO<sub>4</sub>)<sub>2</sub> registered at heating rate of  $10 \text{ K min}^{-1}$  in the temperature range of 300–873 K

is mainly connected with slight changes in water molecule orientations. This aspect cannot be seen and investigated by means of neutron diffraction mainly due to high incoherent cross-section scattering for hydrogen atoms. This is why the neutron powder diffraction method is insensitive for water molecule orientation. This conclusion is compatible to the results obtained by us from single crystal X-ray diffraction measurements. The NPD patterns can be evaluated only qualitatively.

A comparison of the neutron diffraction patterns obtained for [Ca(H<sub>2</sub>O)<sub>2</sub>](ReO<sub>4</sub>)<sub>2</sub> at 295 and 5 K with those theoretically calculated is presented in Fig. 3. The calculations of the ND patterns were performed with FullProf package [18] based on crystal structures data determined

**Fig. 5** TG, DTG and QMS curves for  $[\text{Ca}(\text{H}_2\text{O})_2](\text{ReO}_4)_2$  registered at heating rate of  $10 \text{ K min}^{-1}$  in the temperature range of 310–1500 K

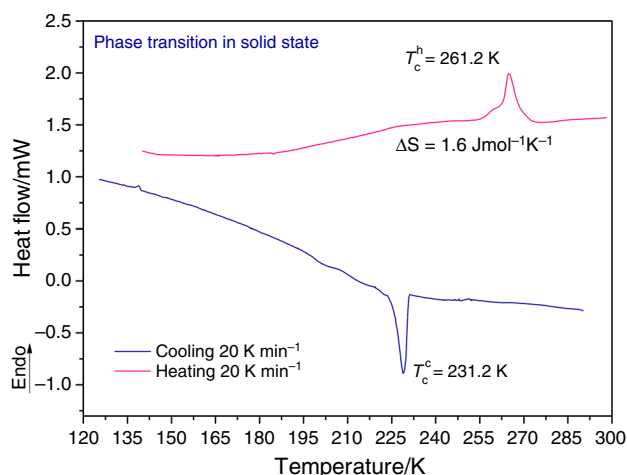
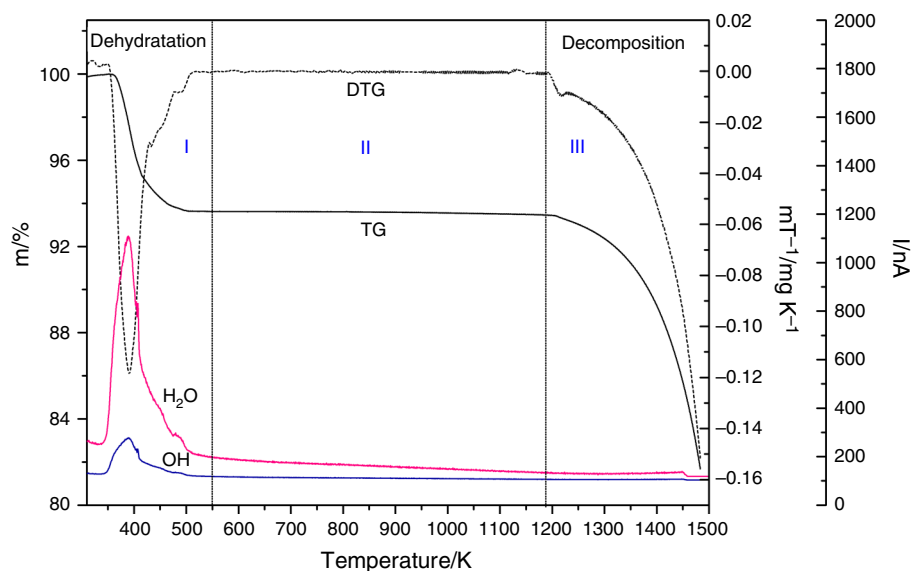


**Fig. 6** DSC curve obtained for  $[\text{Ca}(\text{H}_2\text{O})_2](\text{ReO}_4)_2$  on heating (upper curve) and cooling (lower curve) with a scanning rate of  $20 \text{ K min}^{-1}$

from X-ray single crystal diffraction (XRSCD) measurements for the high-temperature phase. One can see very good agreement between calculated and measured patterns, which confirms proper composition of the investigated sample.

### Thermal behaviour of the title compound (recognition by DSC, TG, QMS)

Figure 4 shows the DSC results obtained in the temperature range of 300–873 K with the scanning rate of  $10 \text{ K min}^{-1}$  for  $[\text{Ca}(\text{H}_2\text{O})_2](\text{ReO}_4)_2$  sample in non-hermetically closed aluminium vessel. This measurement was performed before TG analysis in order to check the stability of the compound and to a qualitative comparison of these results with thermal analysis.

**Table 3** Thermodynamic parameters of the phase transition of  $[\text{Ca}(\text{H}_2\text{O})_2](\text{ReO}_4)_2$

Thermodynamics parameters	$T_c/\text{K}$	$\Delta H \pm \Delta\delta H/\text{J mol}^{-1}$	$\Delta S \pm \Delta\delta S/\text{kJ mol}^{-1} \text{K}^{-1}$
heating	$261.2 \pm 1.1$	$415.4 \pm 23.3$	$1.59 \pm 0.08$
cooling	$231.2 \pm 0.3$	$416.7 \pm 34.5$	$1.80 \pm 0.15$

Three sharp endothermic peaks above 404, 434 and 448 K can be observed in Fig. 4. These peaks can be interpreted as connected with the sample dehydration, which will be proved below by means of the TG results.

Figure 5 presents TG, DTG (derivative TG) and QMS curves recorded for  $[\text{Ca}(\text{H}_2\text{O})_2](\text{ReO}_4)_2$  at a constant heating rate of  $10 \text{ K min}^{-1}$  in the temperature range of 310–1500 K. The following QMS signals were recorded during TG measurements:  $m/z = 17$  and  $18$ —representing  $\text{OH}^-$  and  $\text{H}_2\text{O}$ . The TG, DTG and QMS curves show that the decomposition of the sample proceeds in three main stages (I, II and III). In the first stage (in the temperature range 300–550 K), dehydration of diaquacalcium rhenate(VII) to calcium rhenate(VII) undergoes in one step and all (two) of  $\text{H}_2\text{O}$  molecules are liberated. In the second stage, the investigated anhydrous  $\text{Ca}(\text{ReO}_4)_2$  remains unchanged up to ca. 1180 K. Stage III (above 1185 K) is connected with the decomposition of  $\text{Ca}(\text{ReO}_4)_2$ .

The results obtained in this paper are nearly identical as presented so far in the literature [19]. The dehydration process of  $[\text{Ca}(\text{H}_2\text{O})_2](\text{ReO}_4)_2$  is similar to that one of  $[\text{Mn}(\text{H}_2\text{O})_2](\text{ReO}_4)_2$  [20]. Namely, in the first stage, dehydration takes place in a single step at  $150 \text{ }^\circ\text{C}$  (423 K) and next in the second stage the anhydrous products are formed.

**Table 4** Comparison of the band positions of the infrared (FT-FIR, FT-MIR) spectra and Raman (RS) spectra at two extreme temperatures of measurements for [Ca(H<sub>2</sub>O)<sub>2</sub>](ReO<sub>4</sub>)<sub>2</sub>

Frequencies of vibrations/cm <sup>-1</sup>				Tentative assignments
IR at 9.5/K	IR at 295/K	RS at 87/K	RS at 295/K	
3609 sh				$\nu_{as}(\text{H-O})$
3550 sh	3546 sh	3546 vw		$\nu_{as}(\text{H-O})$
3524 s		3527 vw		$\nu_{as}(\text{H-O})$
3457 s	3457 s	3455 m	3453 w, br	$\nu_s(\text{H-O})$
3397 s	3386 s	3397 m	3392 w, br	$\nu_s(\text{H-O})$
3349 sh				$\nu_s(\text{H-O})$
3240 m	3236 m			$\nu_s(\text{H-O})$
3203 m				$\nu_s(\text{H-O})$
2172 vw				overtones/ combinational bands
2131 vw				
2068 vw				
1635 s	1628 s			$\delta(\text{H-O-H})$
1617 sh				$\delta(\text{H-O-H})$
992 sh	986 sh	992 vs	988 vs	$\nu_s \text{ ReO}_4$
981 sh	981 sh	982 vs	980 vs	$\nu_s \text{ ReO}_4$
963 sh	960 sh			$\nu_s \text{ ReO}_4$
943 sh	945 sh	945 m	942 m	$\nu_s \text{ ReO}_4$
931 vs	926 vs	928 sh	921 m	$\nu_{as} \text{ ReO}_4$
		920 m		$\nu_{as} \text{ ReO}_4$
908 vs		908 sh	908 sh	$\nu_{as} \text{ ReO}_4$
	901 vs	903 m	901 s	$\nu_{as} \text{ ReO}_4$
898 sh				$\nu_{as} \text{ ReO}_4$
643 br, m	646 br, w			$\rho_t(\text{H}_2\text{O})$
602 br, m				$\rho_t(\text{H}_2\text{O})$
563 br, w				$\rho_t(\text{H}_2\text{O})$
507 sh				$\rho_r(\text{H}_2\text{O})$
499 s	494 s			$\rho_r(\text{H}_2\text{O})$
453 m, br	460 m, br			$\rho_t(\text{H}_2\text{O}), \rho_r(\text{H}_2\text{O})$
		365 m		$\delta_d(\text{OReO})$
359 m	357 m	360 m	360 sh	$\delta_d(\text{OReO})$
340 w	341 w	347 m	346 m	$\delta_d(\text{OReO})$
334 sh	334 sh	338 s	336 s	$\delta_d(\text{OReO})$
317 sh	322 sh	324 vw		$\delta_d(\text{OReO})$
306 m	307 m	310 vw	308 vw	H <sub>2</sub> O torsion modes
		304 vw		H <sub>2</sub> O torsion modes
257 br	257 br			$\delta(\text{OCaO})$
204 m	199 m			$\delta(\text{OCaO})$
155 m	152 m			skeletal bending deformations
125 m	119 m			skeletal bending deformations
98 w	95 w			$\nu_L(\text{lattice})$
73 w	76 w	81 w	74 w	$\nu_L(\text{lattice})$
63 w	61 w	68 w	63 w	$\nu_L(\text{lattice})$
58 vw	55 vw			$\nu_L(\text{lattice})$

**Table 4** continued

Frequencies of vibrations/cm <sup>-1</sup>				Tentative assignments
IR at 9.5/K	IR at 295/K	RS at 87/K	RS at 295/K	
44 vw	46 vw			$\nu_L(\text{lattice})$
37 vw	36 vw			$\nu_L(\text{lattice})$

*vs* very strong, *s* strong, *m* medium, *br* broad, *sh* shoulder, *w* weak, *vw* very weak

The temperature ranges of sample transformation were taken from the DSC measurements. They are shifted with respect to TG measurements towards a little bit higher temperatures. The reason is slightly different conditions during measurements. The DSC was performed for sample closed in alumina vessel with micro-hole, whereas the TG investigations were performed in open crucible.

It should be pointed out that the dehydration process of [Ca(H<sub>2</sub>O)<sub>2</sub>](ReO<sub>4</sub>)<sub>2</sub> is similar to [Ba(H<sub>2</sub>O)<sub>3</sub>](ClO<sub>4</sub>)<sub>2</sub> [21], but quite different from the dehydration processes registered for [Ca(H<sub>2</sub>O)<sub>4</sub>](ClO<sub>4</sub>)<sub>2</sub> [22]. In the titled compound, dehydration process occurs simultaneously with melting of the sample, whereas [Ca(H<sub>2</sub>O)<sub>4</sub>](ClO<sub>4</sub>)<sub>2</sub> dissolves in its own coordination water (melts) before dehydration.

Comparing temperatures of ligands lost of [Ca(H<sub>2</sub>O)<sub>2</sub>](ReO<sub>4</sub>)<sub>2</sub> and [Ni(NH<sub>3</sub>)<sub>4,6</sub>](ReO<sub>4</sub>)<sub>2</sub> [4] and [Cd(NH<sub>3</sub>)<sub>4</sub>](ReO<sub>4</sub>)<sub>2</sub> [5], we noticed that they proceed in a similar way. It can be seen that in the case of [Ca(H<sub>2</sub>O)<sub>2</sub>](ReO<sub>4</sub>)<sub>2</sub> the all ligands (H<sub>2</sub>O) are liberated in nearly the same temperature range (300–550 K) same as the NH<sub>3</sub> in [Ni(NH<sub>3</sub>)<sub>4,6</sub>](ReO<sub>4</sub>)<sub>2</sub> (300–590 K) [4] and [Cd(NH<sub>3</sub>)<sub>4</sub>](ReO<sub>4</sub>)<sub>2</sub> (300–600 K) [5]. Anhydrous Ca(ReO<sub>4</sub>)<sub>2</sub> is more stable than nickel and cadmium rhenates(VII).

### Phase transition investigations by DSC

Figure 6 shows the temperature dependencies of the heat flow (DSC curves) obtained on heating (red curve) and on cooling (blue curve) of the [Ca(H<sub>2</sub>O)<sub>2</sub>](ReO<sub>4</sub>)<sub>2</sub>. The heating/cooling rates for the sample were 20 K min<sup>-1</sup>. One distinct anomaly on each of these two DSC curves was registered at:  $T_c^h = 261.2$  K and  $T_c^c = 231.2$  K (where indexes h and c denote heating and cooling of the sample, respectively). These phase transition temperatures were taken as the onset temperature ( $T_{\text{onset}}$ ) for the endothermic peak in the DSC curve response. Thus, the title compound has two solid phases in the temperature range 120–300 K: high-temperature phase (phase I) and low-temperature phase (phase II). The mean values of the enthalpy and

entropy changes in the detected phase transitions are presented in Table 3. The value of entropy change  $\Delta S \approx 1.6 \pm 0.08 \text{ J mol}^{-1} \text{ K}^{-1}$  accompanying these phase transitions suggests also their “order–disorder” mechanism. The presence of 30 K hysteresis of the phase transition temperature at  $T_C$  and sharpness of the anomaly attests that the detected phase transition is of the first-order type.

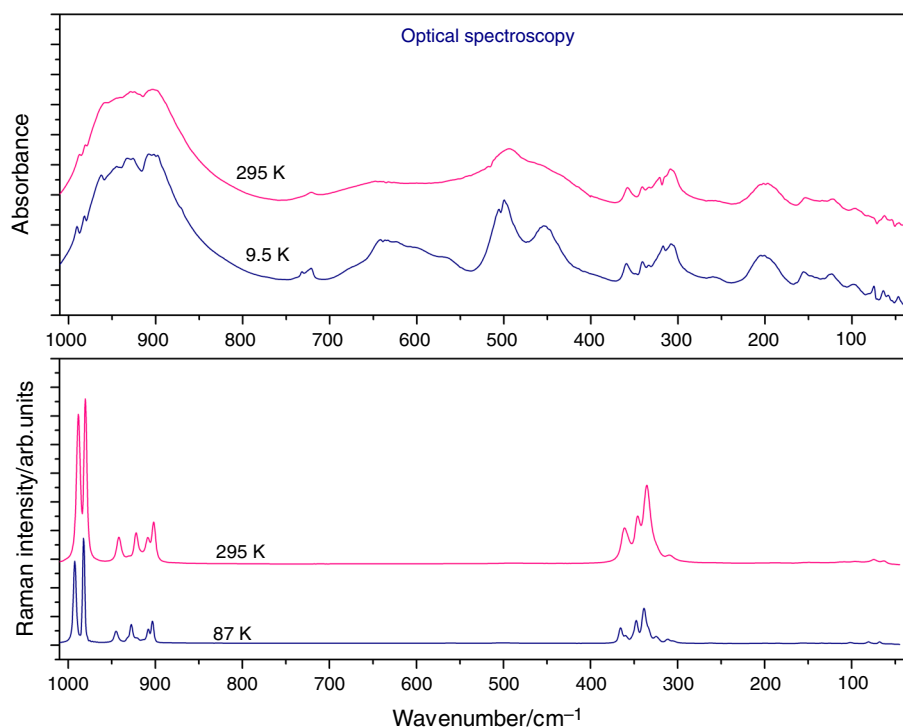
### Vibrational motions and phase transition

Vibrational FT-IR and Raman spectra for  $[\text{Ca}(\text{H}_2\text{O})_2](\text{ReO}_4)_2$  were measured as a function of temperature. The list of the band positions, their relative intensities and tentative assignments are listed in Table 4. The assignments of these vibrations were proposed by comparing their frequencies with the literature data collected for titled compounds and similar ionic aquametal(II) complexes [23, 24] and perrhenate complexes [4, 24, 25]. All characteristic frequencies of  $\text{H}_2\text{O}$  and  $\text{ReO}_4^-$  internal modes were identified. Also some of the bands associated with stretching of Ca–O and bending of the O–Ca–O bonds were observed. These assignments proved that the composition and structure of the investigated compound are correct. According to the group theory, unperturbed  $\text{ReO}_4^-$  anion with  $T_d$  symmetry generates four vibrational modes: fully symmetric stretching  $\nu_1 = \nu_s(\text{ReO})A_1$  at  $971 \text{ cm}^{-1}$ , doubly degenerated asymmetric bending  $\nu_2 = \delta_d(\text{OReO})E$  at  $331 \text{ cm}^{-1}$ , triply degenerated asymmetric

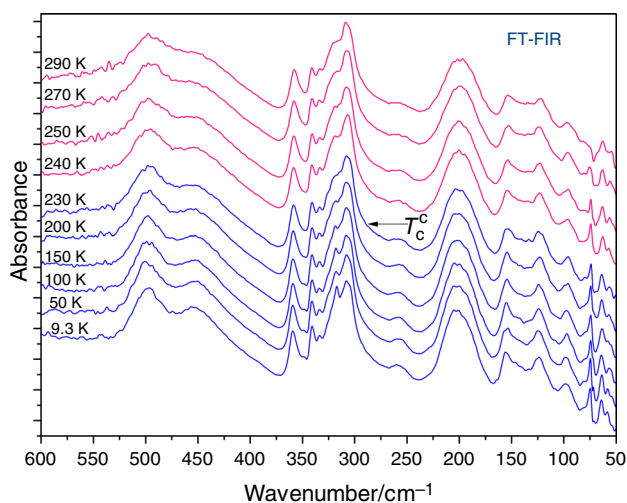
stretching  $\nu_3 = \nu_{as}(\text{ReO})F_2$  at  $920 \text{ cm}^{-1}$  and symmetric bending  $\nu_4 = \delta_d(\text{OReO})F_2$  at  $333 \text{ cm}^{-1}$ . For an isolated  $\text{ReO}_4^-$  anion, all these four modes are RS active and  $\nu_3$  and  $\nu_4$  are IR active only. However, when the high-symmetry structure of the  $\text{ReO}_4^-$  anions is even slightly perturbed, its degenerated vibrational modes may split and some of the inactive modes may become active. Figure 7 presents the comparison of the experimental IR and Raman spectra at two extreme temperatures of measurements in the range of  $1000\text{--}30 \text{ cm}^{-1}$  for  $[\text{Ca}(\text{H}_2\text{O})_2](\text{ReO}_4)_2$ .

Figure 8 shows the FT-FIR spectra of  $[\text{Ca}(\text{H}_2\text{O})_2](\text{ReO}_4)_2$ , within the wave number range  $600\text{--}50 \text{ cm}^{-1}$  registered during the cooling of the sample from 290 to 9.3 K. The spectra marked with pink and blue were registered for the high-temperature (above  $T_C$ ) and the low-temperature (below  $T_C$ ) phases, respectively. The assignment of the chosen IR spectra to the corresponding phase was based on the differential scanning calorimetry (DSC) results. Some interesting changes can be noticed for the far-infrared bands in the range  $600\text{--}50 \text{ cm}^{-1}$  associated with the librational modes of water molecules (twisting  $\rho_t(\text{H}_2\text{O})$  and rocking  $\rho_r(\text{H}_2\text{O})$  modes). During the cooling of the sample, the intensity changes and narrowing of this band can be noticed in the region of the phase transition (PT). Additionally, FT-FIR measurements showed that bands associated with bending  $\delta(\text{OReO})$  deformation modes (wave number between  $360$  and  $317 \text{ cm}^{-1}$ ) narrow continuously with temperature decreasing (see Fig. 8 and Table 4).

**Fig. 7** Comparison of the experimental vibrational IR and RS spectra of  $[\text{Ca}(\text{H}_2\text{O})_2](\text{ReO}_4)_2$  in two extreme temperatures







**Fig. 8** Selected FT-FIR spectra in the wave number range of 600–50 cm<sup>-1</sup> at different temperatures registered at cooling of [Ca(H<sub>2</sub>O)<sub>2</sub>](ReO<sub>4</sub>)<sub>2</sub>. Phase transition temperature registered by DSC also at cooling is indicated by arrow

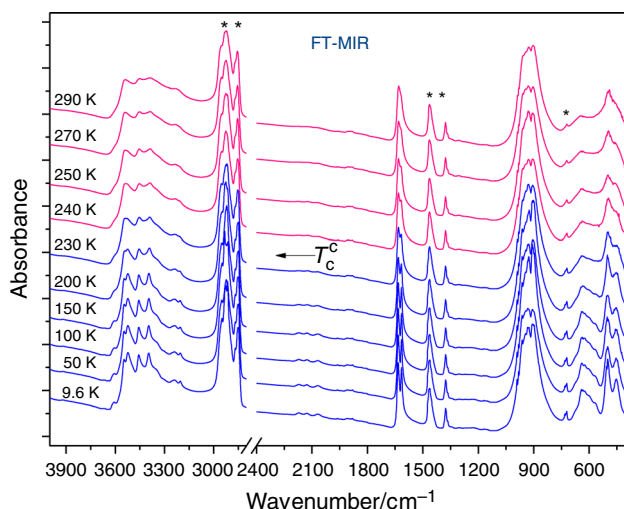


**Fig. 9** Middle-infrared spectra in the wave number ranges 4000–2800 and 2400–400 cm<sup>-1</sup> at different selected temperatures (at cooling of the [Ca(H<sub>2</sub>O)<sub>2</sub>](ReO<sub>4</sub>)<sub>2</sub> sample in Nujol). Phase transition temperature registered by DSC also at cooling is indicated by arrow

The temperature-dependent FT-MIR spectra were also recorded during a cooling of the sample. Figure 9 shows exemplarily the spectra in the wave number ranges: 4000–2800 cm<sup>-1</sup> and 2400–400 cm<sup>-1</sup> at selected temperatures of measurement. Some evident changes in the spectra at the temperature region of the phase transition can be noticed. Namely, apart from the narrowing, the splitting of some bands can be seen below the phase transition. As one can see in Fig. 9, new bands start to appear in the spectra on cooling just after the phase transition temperature (at ca. 230 K) in the wave number range 3700–3300 cm<sup>-1</sup>, connected with the asymmetric and

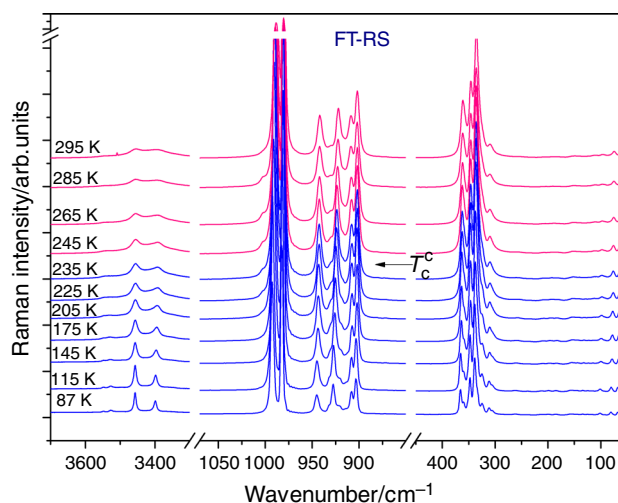


**Fig. 10** Raman spectra in the frequency range of 3700–3300, 1070–850 and 450–50 cm<sup>-1</sup> in selected temperatures (during cooling of the [Ca(H<sub>2</sub>O)<sub>2</sub>](ReO<sub>4</sub>)<sub>2</sub> sample)

symmetric stretching modes ( $\nu_{as}(\text{OH})$  and  $\nu_s(\text{OH})$ ). As one can see in the spectra in Fig. 9, the band at 1628 cm<sup>-1</sup> starts to split into two peaks at 1635 and 1617 cm<sup>-1</sup> on cooling at ca. 240 K (before the phase transition temperature  $T_c$ ).

Figure 10 shows the Raman spectra in the wave number range of 3700–3300, 1070–850 and 450–50 cm<sup>-1</sup> at selected temperatures registered during the cooling of the [Ca(H<sub>2</sub>O)<sub>2</sub>](ReO<sub>4</sub>)<sub>2</sub> sample in the temperature range of 295–87 K. Some interesting changes can be noticed for the bands at ~3392 cm<sup>-1</sup>. This band is associated with the stretching vibration of water molecules  $\nu_s(\text{OH})$ . During the cooling of the sample we can observe narrowing of this band. Moreover, at the lowest temperature of measurement we observe additional bands at wave numbers: 3546 and 3527 cm<sup>-1</sup> associated with stretching mode  $\nu_{as}(\text{OH})$ ; 920 and 365 cm<sup>-1</sup>, 324 cm<sup>-1</sup> connected with the ReO<sub>4</sub><sup>-</sup> anion normal modes  $\nu_{as}(\text{ReO})$  and  $\delta_d(\text{OCIO})$ , respectively.

FT-MIR, FT-FIR and FT-RS measurements analysis for [Ca(H<sub>2</sub>O)<sub>2</sub>](ReO<sub>4</sub>)<sub>2</sub> compound showed that bands associated with H<sub>2</sub>O and ReO<sub>4</sub><sup>-</sup> vibrations modes narrow continuously with temperature decreasing. This suggests that the H<sub>2</sub>O and ReO<sub>4</sub><sup>-</sup> reorientation is slowing down during the cooling of the sample.

## Conclusions

The results obtained in this work and their comparison with the literature data have led us to the following conclusions:

At room temperature, (RT) diaquacalcium rhenate(VII) crystallises in the centrosymmetric monoclinic system (space group I 2/a, No. = 15) with the unit cell parameters:

$a = 18.1302(7) \text{ \AA}$ ,  $b = 7.0722(2) \text{ \AA}$ ,  $c = 14.1882(5) \text{ \AA}$ ,  $\alpha = \gamma = 90^\circ$ ,  $\beta = 119.637^\circ$  and with eight molecules per unit cell ( $Z = 8$ ).

The differential scanning calorimetry (DSC) revealed that diaquacalcium rhenate(VII) exhibits, in the temperature range of 300–120 K, one reversible phase transition at ca.  $T_c^h = 261.2 \text{ K}$  (onset on heating) and  $T_c^c = 231.2 \text{ K}$  (onset on cooling). The thermal hysteresis of the phase transition temperature  $T_c$  equal to  $\sim 30 \text{ K}$  and the heat flow anomaly sharpness suggest that the detected phase transition is a first-order one. The values of the entropy changes ( $1.6 \pm 0.08 \text{ J mol}^{-1} \text{ K}^{-1}$ ) accompanying the phase transition suggest its “order–disorder” mechanism.

The neutron diffraction pattern (ND) at 295 K is nearly exactly the same as that at 5 K, which implies that the phase transition at  $T_c^h = 261.2 \text{ K}$  has not structural character. The space group (I 2/a, No = 15) is the same for high- and low-temperature phases. However, there are small changes in water molecule orientation and torsion angles in the structure.

Using vibrational spectroscopy methods (IR and RS), all characteristic wave numbers of the internal vibrations of  $\text{H}_2\text{O}$  and  $\text{ReO}_4^-$  and external vibrations connected with the stretching of Ca–O and the bending of O–Ca–O bonds in  $[\text{Ca}(\text{H}_2\text{O})_2]^{2+}$  cations were detected. There was a general agreement between the wave numbers observed in this work and in the literature. Characteristic changes in band wave numbers in the FT-IR and Raman spectra were clearly observed. The appearing (splitting) of some infrared and Raman bands near temperature  $T_c$  suggests that the observed phase transition is probably connected with the change in the site symmetry of the complex cation or anion. FT-MIR, FT-FIR and FT-RS measurements showed that bands associated with  $\text{H}_2\text{O}$  and  $\text{ReO}_4^-$  vibrations modes narrow continuously with temperature decreasing.

The thermal decomposition process of the  $[\text{Ca}(\text{H}_2\text{O})_2](\text{ReO}_4)_2$  proceeds in the three main stages. In the first stage (300–550 K), dehydration of  $[\text{Ca}(\text{H}_2\text{O})_2](\text{ReO}_4)_2$  to anhydrous  $\text{Ca}(\text{ReO}_4)_2$  undergoes in one step and all of  $\text{H}_2\text{O}$  molecules are liberated. In the second stage, the investigated anhydrous  $\text{Ca}(\text{ReO}_4)_2$  remains unchanged up to ca. 1180 K. Stage III (above 1185 K) is connected with the decomposition of  $\text{Ca}(\text{ReO}_4)_2$ .

**Acknowledgements** The infrared absorption (FT-MIR and FT-FIR) researches were carried out with the equipment purchased thanks to the financial support of the European Regional Development Fund in the framework of the Polish Innovation Economy Operational Program (contract no. POIG.02.01.00-12-023/08). The project was supported by the grant of the Polish Plenipotentiary to JINR and JINR Directorate from 25.02.2014, Nr 118 p.7.

**Open Access** This article is distributed under the terms of the Creative Commons Attribution 4.0 International License (<http://creativecommons.org/licenses/by/4.0/>), which permits unrestricted use,

distribution, and reproduction in any medium, provided you give appropriate credit to the original author(s) and the source, provide a link to the Creative Commons license, and indicate if changes were made.

## References

- Migdał-Mikuli A, Hetmańczyk J, Nitek W, Mikuli E, Hetmańczyk Ł. Phase transitions in  $[\text{Ca}(\text{H}_2\text{O})_4](\text{ClO}_4)_2$  studied by differential scanning calorimetry, X-ray single crystal diffraction and neutron powder diffraction. *J Mol Struct.* 2008;891:233–41.
- Hetmańczyk J, Hetmańczyk Ł, Migdał-Mikuli A, Mikuli E, Weselucha-Birczyńska A. Raman light scattering, infrared absorption and DSC studies of the phase transition and vibrational and reorientational dynamics of  $\text{H}_2\text{O}$  ligands and  $\text{ClO}_4^-$  anions in  $[\text{Ba}(\text{H}_2\text{O})_3](\text{ClO}_4)_2$ . *J Raman Spectrosc.* 2012;43:1118–25.
- Hetmańczyk J, Hetmańczyk Ł, Migdał-Mikuli A, Mikuli E. Vibrational and reorientational dynamics, crystal structure and solid–solid phase transition studies in  $[\text{Ca}(\text{H}_2\text{O})_6]\text{Cl}_2$  supported by theoretical (DFT) calculations. 2016. doi:10.1002/jrs.4863.
- Hetmańczyk Ł, Hetmańczyk J. Comparison of vibrational dynamics, thermal behaviour, and phase transition in  $[\text{Ni}(\text{NH}_3)_4](\text{ReO}_4)_2$  and  $[\text{Ni}(\text{NH}_3)_6](\text{ReO}_4)_2$ . *J Thermal Anal Calorim.* 2015;119:1415–28.
- Hetmańczyk Ł, Hetmańczyk J. Phase transition, thermal dissociation and dynamics of  $\text{NH}_3$  ligands in  $[\text{Cd}(\text{NH}_3)_4](\text{ReO}_4)_2$ . *Spectrochim Acta A.* 2016;164:24–32.
- Baur WH, Kassner D. The crystal structure of  $\text{Ca}(\text{ReO}_4)_2 \cdot 2\text{H}_2\text{O}$ . *J Solid State Chem.* 1992;100:166–9.
- Matveeva RG, Ilyukhin VV, Varfolomeev MB, Belov NV. *Soviet Physics – Doklady.* 1980;252:92–102.
- Picard JP, Besse JP, Chevalier R. Structure cristalline de  $\text{Ca}(\text{ReO}_4)_2 \cdot 2\text{H}_2\text{O}$ . *J Solid State Chem.* 1987;69:380–4.
- Otwinowski Z, Minor W. *Macromolecular crystallography.* In: Carter CW Jr, Sweet RM, editors. *Methods in enzymology*; part A. Orlando:Academic; 1997. Vol. 276, p. 307–26.
- Altomare A, Cascarano G, Giacovazzo C, Guagliardi AJ. Completion and refinement of crystal structures with SIR92. *J Appl Crystallogr.* 1993;26:343–50.
- Sheldrick GM. SHELXL-97 programs for crystal structure analysis (Release 97-2); Institut für Anorganische Chemie der Universität, Tammanstrasse 4, D-3400 Göttingen, Germany. 1998.
- Hetmańczyk J, Hetmańczyk Ł, Migdał-Mikuli A, Mikuli E. Vibrational and reorientational motions of  $\text{H}_2\text{O}$  ligands, phase transition and thermal properties of  $[\text{Sr}(\text{H}_2\text{O})_6]\text{Cl}_2$ . *Spectrochim Acta A.* 2013;115:504–10.
- Natkaniec I, Chudoba D, Hetmańczyk Ł, Kazimirov VY, Krawczyk J, Sashin IL, Zalewski S. Parameters of the NERA spectrometer for cold and thermal moderators of the IBR-2 pulsed reactor. *J Phys Conf Ser.* 2014;554:012002.
- Hetmańczyk J, Hetmańczyk Ł, Migdał-Mikuli A, Mikuli E, Florek-Wojciechowska M, Harańczyk H. Vibrations and reorientations of  $\text{H}_2\text{O}$  molecules in  $[\text{Sr}(\text{H}_2\text{O})_6]\text{Cl}_2$  studied by Raman light scattering, incoherent inelastic neutron scattering and proton magnetic resonance. *Spectrochim Acta A.* 2014;124:429–40.
- Wells AF. *Structural inorganic chemistry.* 5th ed. Oxford: Oxford University Press; 1984.
- Bouhali A, Trifa C, Bouacida S, Boudaren C, Bataille T. Poly[[ $\mu$ -aqua-tetraaquabis( $\mu$ -2-hydroxy-4-oxocyclobut-1-ene-1,3-diolato)strontium] hemihydrate]. *Acta Crystallogr E.* 2011;E67:m1130–1.
- CrystalMaker Software Ltd: crystal and molecular structures, modelling, visualisation software plus diffraction pattern simulation for Mac OS X and Windows. <http://www.crystallmaker.com/crystallmaker/>.

18. Rodriguez-Carvajal J. Recent advances in magnetic structure determination by neutron powder diffraction. *Phys B*. 1993;192:55–69.
19. Teterin EG, Zaitseva LL, Samsonov VE, Aksenenko AV. IR and proton NMR spectral study of calcium pertechnetate and perhenate. *Russ J Inorg Chem*. 1986;8:2012–6.
20. Butz A, Mieke G, Paulus H, Strauss P, Fuess H. The crystal structures of Mn(ReO<sub>4</sub>)<sub>2</sub>·2H<sub>2</sub>O and of the anhydrous perhenates M(ReO<sub>4</sub>)<sub>2</sub> of divalent manganese, cobalt, nickel, and zinc. *J Solid State Chem*. 1998;138:232–7.
21. Migdał-Mikuli A, Hetmańczyk J, Mikuli E, Hetmańczyk Ł. Thermal behaviour of polycrystalline [Ba(H<sub>2</sub>O)<sub>3</sub>](ClO<sub>4</sub>)<sub>2</sub> and [Ba(NH<sub>3</sub>)<sub>4</sub>](ClO<sub>4</sub>)<sub>2</sub>. *Thermochim Acta*. 2009;487:43–8.
22. Migdał-Mikuli A, Hetmańczyk J. Thermal behavior of [Ca(H<sub>2</sub>O)<sub>4</sub>](ClO<sub>4</sub>)<sub>2</sub> and [Ca(NH<sub>3</sub>)<sub>6</sub>](ClO<sub>4</sub>)<sub>2</sub>. *J Thermal Anal Calorim*. 2008;91:529–34.
23. Lutz HD. Bonding and structure of water molecules in solid hydrates: correlation of spectroscopic and structural data. *Struct Bond*. 1988;69:97–125.
24. Nakamoto K. Infrared and Raman spectra of inorganic and coordination compounds. 5th ed. New York: Wiley-Interscience Publication; 1997.
25. Gassman PL, McCloy JS, Soderquista ChZ, Schweiger MJ. Raman analysis of perhenate and pertechnetate in alkali salts and borosilicate glasses. *J Raman Spectrosc*. 2014;45:139–47.